Image Processing Techniques for Satellite Terrain Analysis

Kanar Sami, Esraa Abd Alsalam and Mohammed Hazim Alkawaz
Department of Computer Science, College of Education for Pure Sciences, University of Mosul, 41002 Nineveh, Iraq
lamarsafwan111@uomosul.edu.iq, esraa.altoni@uomosul.edu.iq, mohammed.ameen@uomosul.edu.iq

Keywords: Mean Absolute Deviation, Satellite Data, Contourlet Transform, Digital Image Processing, Standard Deviation.

Abstract: The contourlet transform had been used in the multimedia processing works and processes of compression, encoding, and steganography of audio and with images and video data. In the present study, satellite images recorded with the Sentinel-2 were used to investigate the drainage systems in the Mosul Dam Basin. The high-frequency coefficients were removed selectively and reconstructed with the remaining coefficients to analyse how frequency loss affect the quality of images. The contribution of low-frequency components to reconstructed images was further determined in numerical terms measured by mean squared error and the Signal to noise ratio, normalized root mean square deviation (NRM), and correlation coefficient. Across some decomposition levels, results from experiments on bands 1, 2 and 4 demonstrated that low NRM values, high SNR values, and correlation coefficients converged into unity, suggesting a reasonable estimation accuracy. The cut off values for frequency elimination were taken using standard deviation (STD) and median absolute deviation (MAD) criteria. The data supported the effectiveness of the contourlet-based frequency assessment which evaluated the influence of removing coefficients on satellite image characteristics for the following scenarios: data compression, edge detection, noise removal, and terrain feature extraction for drainage pattern maps in the Mosul Dam region.

1 INTRODUCTION

Despite the importance of satellite imagery and image enhancement techniques in remote sensing applications [1], [2], there is a clear lack of studies that quantitatively assess the impact of selective frequency component removal on the interpretation of geomorphological features, particularly when extracting drainage systems. Most previous studies in image enhancement and frequency processing have focused on improving visual quality or overall reconstruction performance [3]-[5], without analyzing the extent to which the spatial structure of topographic features is preserved when certain frequency components are removed according to specific statistical criteria. To address this gap, this study proposes a framework based on the contourlet transform, which has proven effective in numerous image processing applications [3], [5]. This framework selectively removes high-frequency components based on statistical thresholds derived from standard deviation (STD) and median absolute deviation (MAD). Images are then reconstructed and quantitatively evaluated using MSE, SNR, NRM, and correlation coefficients to measure the contribution of low-frequency components to the preservation of drainage patterns. The key contributions of this study are:

1) Providing a quantitative assessment of the impact of high-frequency removal on the accuracy of geomorphological interpretation in remote sensing images.
2) Employing an objective statistical approach to determine cutoff thresholds based on frequency analysis concepts [3].
3) Analyzing the preservation of drainage patterns across multiple levels of analysis using a framework based on frequency processing techniques [4], [5].

The research consists of the following sections: Section two reviews previous studies, section three presents the proposed methodology, section four presents the results and analysis, while section five includes the conclusions and future recommendations.

2 RELATED WORKS

A lot of image processing applications, like image compression, noise reduction, haze removal, and security systems, utilize frequency-domain transformations that enable the independence of high and low frequency operations [1]. Given the poor sensitivity of the human visual system to high-frequency elements of an image (e.g., its edges), most image processing methods center their processing around these frequencies. However, the general one-dimensional transforms adopted in image processing, e.g., the Fourier and Wavelet transforms, have limitations regarding the geometric structure and edge rendering of images [2]. In addition, selective excision of certain low-frequency components will make these images under foggy/hazy conditions more visible [3]. A new study was proposed which was based on the study about removing high-frequency coefficients from contourlet-transformed images. They studied reconstruction of images after discarding specific high frequency components and how the levels of decomposition affect. Performance measurements for the influence of frequency removal were measured for MSE, PSNR, SSIM, and other performance metrics. [4] explored noise avoidance methods at multiple spatial resolutions with Sentinel-2 satellite imagery. In the work they compared four spatial domain filtering approaches against frequency domain thresholding methods, using wave-based Contourlet and Curvelet transforms. Based on the quality assessment, the hard thresholding with the Curvelet transform gave the best results. Additionally, [5] proposed a single image dehazing method based on the high-resolution non-subsampled contourlet transform (HRNSCT). In this approach, the non-subsampled contourlet transform (NSCT) is applied to decompose noisy and hazy color images into low-frequency and high-frequency directional sub bands. Haze is removed only from the low-frequency sub bands to prevent amplification of noise in high-frequency regions. The technique integrates prior color attenuation with dark channel pre-attenuation to estimate the transmission map, which is subsequently used to refine the low-frequency sub bands across all color channels. Despite the widespread use of frequency-domain transformations in image enhancement, noise reduction, and fog treatment, most previous studies have focused primarily on improving optical quality and restoration performance. Insufficient attention has been paid to the systematic quantitative study of the selective removal of frequency components and its impact on the interpretation of geomorphological features in satellite imagery. In particular, the effect of removing high-frequency parameters on characterizing drainage systems using specific statistical criteria for cut-off boundaries remains largely unexplored. This research gap motivates the current study, which aims to systematically evaluate the role of frequency components in extracting topographic features within the Mosul Dam basin.

3 STUDY AREA

Mosul Dam Lake is an Iraqi reservoir formed by the Mosul Dam, surrounded by natural landscapes and recognized for its economic and touristic significance. The lake extends longitudinally along the Tigris River between longitudes (40°55′–40°86′) and latitudes (27°50′–32°00′), with an approximate length of 45 km and a width ranging from 2 to 14 km. It covers a surface area of about 380 km² at an elevation of 330 m above sea level. Ten valleys flow into the lake, as illustrated in Figure 1 [6]. About 50 km north of Mosul, as part of Nineveh Governorate of northern Iraq, is the Mosul Dam along the course of the Tigris River [7], [8]. The Tigris River within the Mosul region is classified as a gravel-bed river, which generally comprises two layers: a coarse surface layer consisting mainly of gravel, and an underlying subsurface layer containing a mixture of gravel, sand, and fine materials [9].

Figure 1: Mosul Dam.

4 MATERIALS AND METHODS

The Copernicus Sentinel-2 mission consists of two polar-orbiting satellites operating in a sun-synchronous orbit and phased 180° apart. This configuration enables high temporal resolution, providing global land coverage every 10 days with a single satellite, or every 5 days when both satellites are operational, depending on latitude and imaging conditions.

Sentinel-2 supplies overall data for the purpose of environmental measurements, including objectives of the mission, the specific satellite and ground segment descriptions, and applications in monitoring terrestrial and thematic surface variations [10]. Every Sentinel-2 satellite has a Multispectral Instrument (MSI) featuring 13 spectral bands that cover the visible, near-infrared (NIR), and shortwave infrared (SWIR) regions. The spectral bands have spatial resolutions ranging from 10 meters to 60 meters depending on their wavelength and function. A detailed list of the Sentinel-2 spectral bands is presented for each wavelength and spatial resolutions in Table 1 [11].

Table 1: Sentinel wavelengths and resolutions.

Sentinel-2	Bands	Wavelength (µm)	Resolution (m)
Coastal aerosol (CA)	B1	0.443	60
Blue	B2	0.490	10
Green	B3	0.560	10
Red	B4	0.665	10
Vegetation Red Edge (VRE)	B5	0.705	20
Vegetation Red Edge (VRE)	B6	0.740	20
Vegetation Red Edge (VRE)	B7	0.783	20
NIR	B8	0.842	10
Vegetation Red Edge (VRE)	B8A	0.865	20
Water vapour	B9	0.945	60
SWIR – Cirrus	B10	1.375	60
SWIR	B11	1.610	20
SWIR	B12	2.190	20

5 PREPROCESSING METHOD

Sentinel-2 satellite data for the Mosul Dam area in the city of Mosul were utilized in this study, specifically bands 1, 2, and 3, as illustrated in Figure 2.

Figure 2: Three bands of sentinel satellite data.

The widespread use of images has increased dramatically with technological improvement in recent years in many fields, such as medicine, space exploration, education, research, and communications. Therefore, knowledge of image processing and enhancement principles has become essential in many scientific and practical applications. The rapid change in this field often raises serious issues for researchers trying to improve degraded images or images that were affected by noise. Therefore, this research focuses on developing an advanced algorithm aimed at improving the quality and visualization of images to better serve the intended analytical and practical purposes.

Before applying the proposed enhancement techniques, several preprocessing steps were performed to prepare the satellite imagery for analysis, as summarized below:

1) Correction of the satellite data, since satellite images are often captured with geometric inclination or distortion, as illustrated in Figure 3.
2) Determining the study area from the full satellite dataset, followed by cropping and resizing it according to the study requirements, as shown in Figure 4.

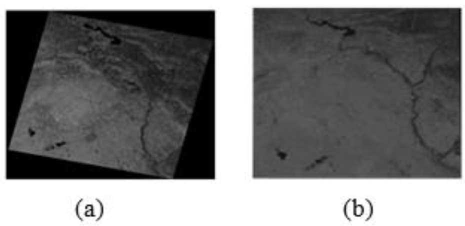

Figure 3: Satellite image correction process: a) before correction; b) after correction.

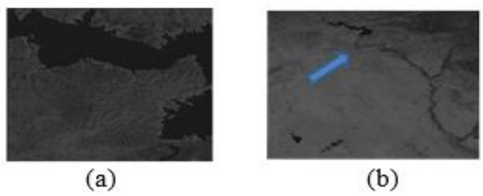

Figure 4: Study area extraction process: a) selection of the study area; b) cropped study area with the required size.

Both noise removal and smoothing algorithms play a vital role in enhancing image clarity. In this study, the linear stretch equation was applied to expand the image histogram and improve the visual quality of grayscale images. This enhancement increases the visibility of image details by adjusting brightness levels according to pixel intensity distribution. High image clarity is achieved when most pixel values are concentrated near high illumination levels (r → 255), moderate clarity when pixel intensities are centered in the mid-range, and low clarity when values are concentrated near low illumination levels (r → 0). Especially in low contrast images, it is useful, as poor distinction in brightness may result in the identification of objects and their spatial relation and relevance. Linear contrast stretching allows for the visual inspection of both the low brightness and high brightness data by adjusting the values of pixel intensity. For the linear stretch algorithm, the image should be converted into an 8-bit grayscale image with the pixels from 0 to 255, and then it will be presented in the histogram. The histogram shows the frequency of each of the gray levels from a minimum intensity value (OMIN) to a maximum intensity value (OMAX) [12]. A linear stretch is used on the graph as displayed in Figure 5.

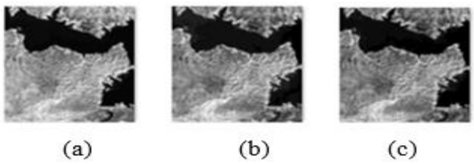

Figure 5: Results of linear contrast stretching for different spectral bands: a) band 1; b) band 2; c) band 4.

6 PROPOSED METHOD

As per Do and Vetterli [13], the Contourlet Transform is another multiscale/multi-directional image decomposition method based on the Laplacian Pyramid (LP) and Directional Filter Banks (DFB). The input image is divided into four principal parts: LL (Low-Low), LH (Low-High), HL (High-Low), and HH (High-High). At each level of the Laplacian Pyramid, the high-frequency components (LH, HL, HH) are processed through the directional filter bank, while the low-frequency component (LL) is recursively passed to the next level of the Laplacian pyramid. This procedure is executed at different levels and along different directions, facilitating the image-based multi-scale and directional image representation [14], [15]. The Contourlet Transform has been widely applied in image processing for tasks such as data extraction, image enhancement, feature extraction, and image correction. Its ability to capture both edge and directional information makes it particularly effective for high-quality image analysis [16]. The first band of the satellite data (b1) of the Sentinel satellite was taken and the contourlet transformation was applied according to the following steps:

6.1 Threshold Methods

The impact of eliminating high frequencies use the threshold method and the application of contourlet transformation in satellite images. The removal of contourlet transformation coefficients for bands of satellite pictures has been addressed using a variety of threshold techniques. For all blocks passing at each level, these thresholds can be used. In this study, two threshold statistic approaches are contrasted.

6.2 Accuracy Measurement

To evaluate the effectiveness and reliability of the proposed image enhancement method, several statistical and signal-quality metrics were employed. These measures assess dispersion, reconstruction quality, similarity, and noise reduction performance between the original and processed images. The selected evaluation metrics are described as follows:

1) The standard deviation is a measure of an array of data dispersed after its mean. The absolute variance of the distribution is measured. Therefore, the deviation and its size from the mean increase with increasing dispersion or variance. The standard deviation is also known as the deviation of a rectangular root mean, because it represents the square root of the squared deviations from the arithmetic mean [17] as shown in (1).

$$std = \sqrt{\left(\frac{\sum_{i=1}^{n} \quad (xi-\underline{x})}{n-1}\right)}. \qquad (1)$$

2) Mean Absolute Deviation (MAD) For forecasting, the measure of Mean Absolute Deviation (MAD) is used to measure accuracy. The MAD scale is considered one of the scales that is characterized by non-success of the current prediction, as well as creating a next round with more accuracy and more correctness of prediction [18]. MAD is defined as the average distance between the mean of a set of numbers, as shown in (2):

$$MAD = median\ |xi - median(xi)|. \qquad (2)$$

3) Signal-to-Noise Ratio (SNR): This metric represents the ratio of the speech signal value to the noise energy [19], measured as shown in.

$$snr = 10\ log10\ \frac{\sigma x^2}{\sigma y^{2.}} \quad (3)$$

where $x$is the original signal and y is the post-processing signal.

4) Normalized Root Mean Square Division (NRM). This is a well-known method for measuring the performance of models, as it is represented by comparing data with groups and models of different scales, as shown in (4).

$$RSMD = \sqrt{\frac{\sum_{t=1}^{T} \blacksquare (y_t - x_t)^2}{T}}, \quad (4)$$

where y is the new sign and x is the reconstructed sign. Next the NRM can be measured by (5).

$$RMSD = \frac{RSMD}{Y_{MINE} - X_{MINE}}. \quad (5)$$

5) The correlation: It is an sign of the correlation among the variables. like signal (x, y) in (6) [20]:

$$correlayion(x, y) = \frac{cov(x,y)}{\partial x \partial y}, \quad (6)$$

where (∂x ∂y): standard division of (x, y).

6.3 Proposed Work Steps

The proposed algorithm can be summarized in the following steps:

1) Read the input image.
2) Analyze the image using the Contourlet Transform, decomposing it into high and low-frequency coefficients.
3) Perform contourlet transformation at level N using the directional filter bank.
4) Remove selected high-frequency coefficients by setting them to zero based on statistical criteria (standard deviation, STD, or median absolute deviation, MAD).
5) Reconstruct the image from the modified coefficients.
6) Evaluate performance by comparing the reconstructed image with the original using standard image quality metrics.

6.4 Applying the Algorithm to Digital Images

The contourlet algorithm was applied to the three Sentinel satellite bands (B1, B2, and B4) through a multilevel frequency decomposition process. The same processing steps were performed for each band; however, Band 1 (Coastal Aerosol) is presented here as a representative example. The analysis was conducted using three decomposition levels to separately examine low- and high-frequency components, as described below:

1) The Band 1 image (B1) was input into the contourlet transform and decomposed into three levels for analysis of low- and high-frequency information. Each decomposition level contains a number of image blocks representing different directional frequency components.
2) The standard deviation was calculated for each block at every decomposition level separately, as illustrated in Figure 6.

7 RESULTS

The research results are divided into two stages. The first stage includes the results obtained using statistical measures. The second stage includes displaying the retrieved satellite images by reconstructing the deleted high-frequency contours.

7.1 Stage 1 (Statistical Metrics)

Accuracy measures (MSE, PSNR, NRM, SNR, CORR) have been used to measure the quality of the image with omitted frequencies based on two measures (STD, MAD) at levels 1, 2, and 3, and for all blocks in the satellite images for three bands 1, 2, and 4, as shown in Tables 2 and 3, respectively.

Figures 7, 8, and 9 have been constructed using three-dimensional models of graphical charts to illustrate statistical measures (STD) and the extent of the effect of deleting frequencies on the images. Figures 10, 11 and 12, on the other hand, have been constructed using three-dimensional models of graphical charts to illustrate statistical measures (MAD).

In Table 4, a numerical comparison is presented between the mean squared error (MSE) values resulting from the application of standard deviation (STD) and mean absolute deviation (MAD) to determine the limits of high-frequency removal in satellite imagery. This comparison is part of evaluating the effect of removing high-frequency parameters within the contour transform on image reconstruction quality.

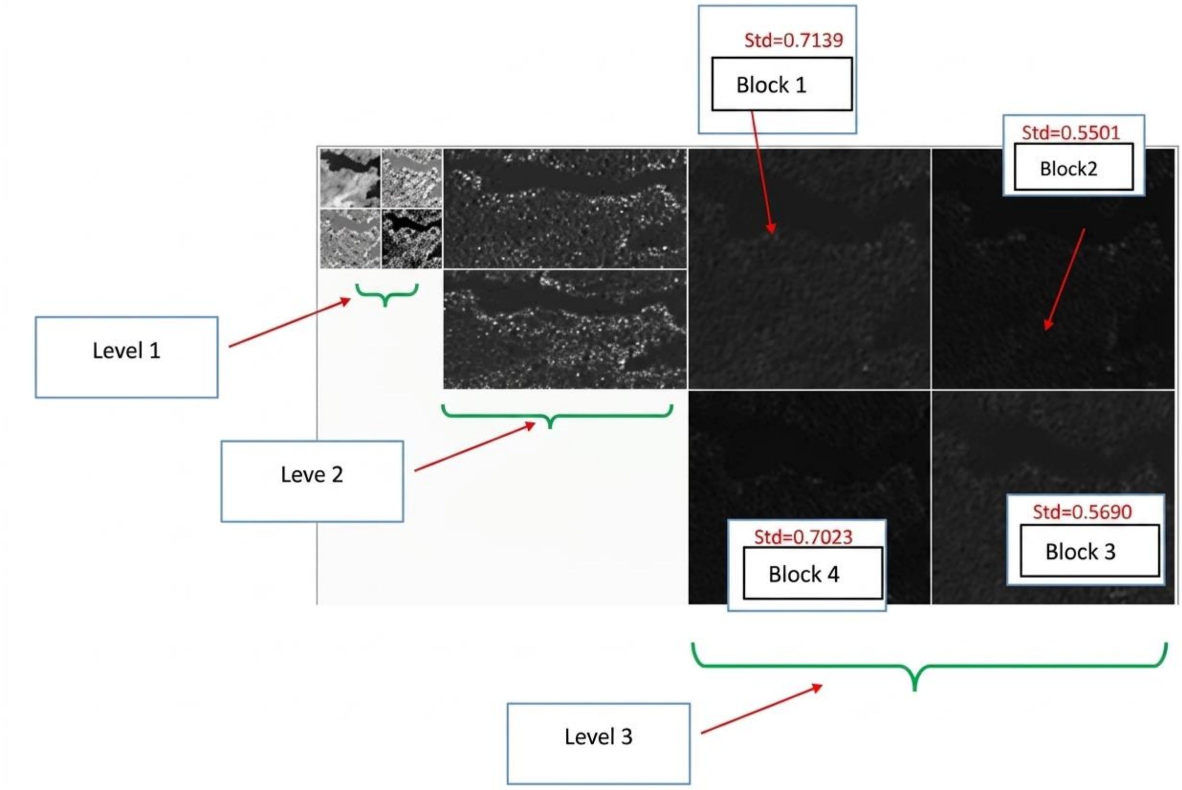

Figure 6: The contourlet algorithm.

Table 2: Elimination frequency for Sentinel satellite data image for the three levels baste of STD.

Band No.	n.Level	MSE	PSNR	NRM	SNR	CORR
Band 1	L- 3	97.8945	28.2232	0.0160	42.0157	0.9354
	L- 2	101.1248	28.0822	0.0160	42.0124	0.8954
	L- 1	105.6954	27.8902	0.0161	41.9981	0.8577
Band 2	L- 3	0.9730	48.2495	0.00010806	63.7287	0.9870
	L- 2	3.2483	43.0142	0.00013525	62.7539	0.9522
	L- 1	5.2433	40.9347	0.00020764	60.8923	0.9228
Band 4	L- 3	2.1621	44.7820	0.00007591	65.2623	0.9946
	L- 2	10.2113	38.0400	0.00007970	65.0503	0.9735
	L- 1	15.7487	36.1584	0.00016355	61.9288	0.9588

The results show that Band 1 at Level 3 performed best according to the MAD criterion, recording the lowest MSE value (0.9861), indicating that choosing a cut value based on MAD leads to better retention of low-frequency information and reduced loss of important image characteristics, especially those related to water drainage patterns. Although Band 2 at the same level showed the lowest STD MSE value (0.9730), the corresponding MAD value was higher, indicating that the STD criterion may be more stable estimate of the effect of removing high-frequency coefficients. These results confirm that low NRM values, high SNR, and a near-unit correlation coefficient reflect good estimation accuracy at certain analysis levels. Therefore, adopting the MAD criterion for determining the frequency removal threshold provides a better balance between error reduction and preserving the spectral and spatial characteristics of the image, thus enhancing the efficiency of data compression, edge detection, noise reduction, and topographic feature extraction applications in the Mosul Dam basin.

Table 3: Elimination frequency for Sentinel satellite data image for the three levels baste of MAD.

Band No.	n.Level	MSE	PSNR	NRM	SNR	CORR
Band 1	L- 3	0.9861	48.1915	0.00010165	63.9943	0.9812
	L- 2	2.6321	43.927	0.00012364	63.1440	0.9367
	L- 1	4.2759	41.8206	0.00021863	60.6683	0.8968
Band 2	L- 3	1.0536	47.9040	0.000094117	64.3287	0.9867
	L- 2	3.3619	42.8650	0.00011120	63.6045	0.9511
	L- 1	5.3938	40.8078	0.00021864	38.5411	0.9170
Band 4	L- 3	2.0095	45.1000	0.00006189	66.1488	0.9950
	L- 2	11.2728	37.6105	0.00006500	65.9359	0.9709
	L- 1	16.2896	36.0117	0.00018434	61.409	0.9576

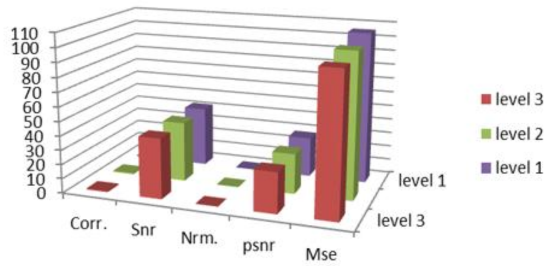

Figure 7: Statistical metrics for satellite images band1using STD.

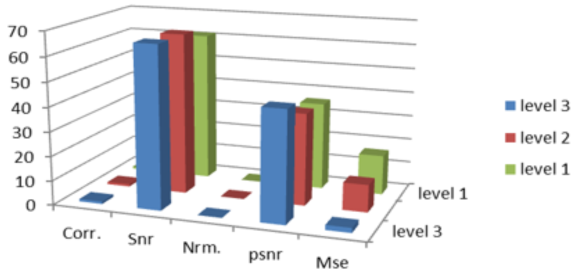

Figure 10: Statistical metrics for satellite images band1 using MAD.

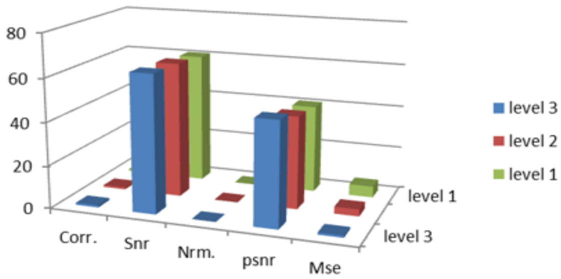

Figure 8: Statistical metrics for band2 satellite images using STD.

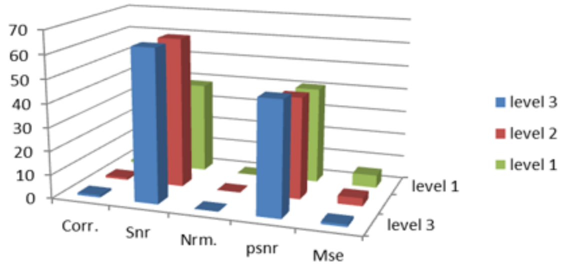

Figure 11: Statistical metrics for satellite images band2 using MAD.

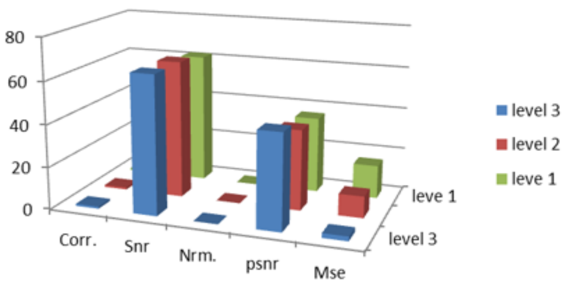

Figure 9: Statistical metrics for band4 satellite images using STD.

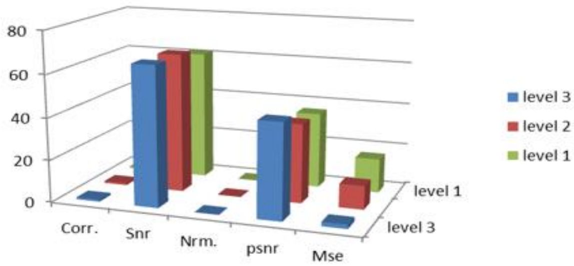

Figure 12: Statistical metrics for satellite images band4 using MAD.

Table 5 presents a comparison that demonstrates the effectiveness and superiority of our method over related studies

7.2 Stage 2 (Image Reconstruction)

At this stage, the satellite images have been reconstructed, as shown in Table 6, which shows the retrieved satellite images using the reconstruct contourlet for bands (1, 2, and 4) for the three levels, adopting the STD scale.

Table 4: Comparison was MAD & STD with each level.

Band no.	Level no.	MSE (STD)	MSE (MAD)
1	3	97.8945	0.9861
2	3	0.9730	1.0536
4	3	2.1621	2.0095

Table 5: A Comparison of the best results of MSE, PSNR of other works with the best result obtained.

REF	PSNR	MSE
[8]	27.000	20.000
[9]	30.000	0.0008
[19]	23.8473	--
[20]	28.000	---
Proposed work	48.1915	0.9861

8 CONCLUSIONS

The experimental results demonstrate that the median absolute deviation (MAD) outperforms the standard deviation (STD) at decomposition level 3 for Band 1 and Band 4, whereas STD achieves superior performance in Band 2. The results indicate that the performance of a statistical approach is band-dependent and depends on frequency characteristics of the original image elements. It emphasizes how high-frequency coefficients are crucial for image quality and reconstruction. Since high-frequency elements hold essential details and edge information and they should be properly modeled and preserved, they can greatly improve reconstruction accuracy. The study verifies that optimizing the treatment of high-frequency coefficients enhances the quality of the image, thereby benefiting a wide range of image processing and analysis applications. The study demonstrated that contour transformation is effective in analyzing satellite imagery for geomorphological purposes. It has also shown that statistically, high-frequency deletion does not significantly affect the representation of drainage systems at certain analysis levels. The results confirm that low-frequency components are essential for preserving the image's topographic structure.

Table 6: Image reconstruction based on STD.

	Band 4 (RED)	Band 2 (Blue)	Band 1 (Coastal aerosol)
Original image	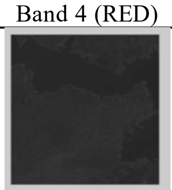		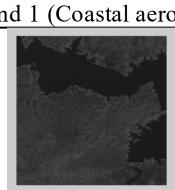
Blocks 1, 2, 3,4 have been zeroed in Level 3	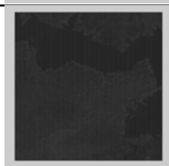	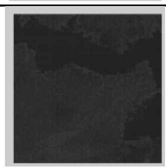	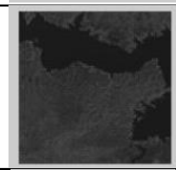
Blocks 1, 2 have been zeroed in Level 2	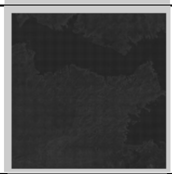	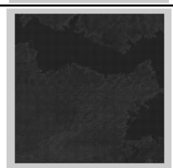	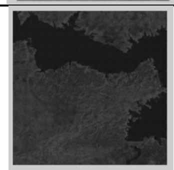
Blocks 1, 2, 3,4 have been zeroed in Level 1		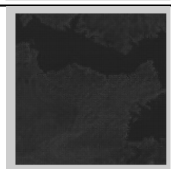	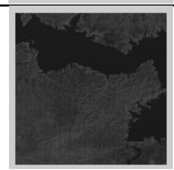

ACKNOWLEDGMENTS

The authors are grateful to the computer science department at the COEFPS at the university of Mosul for their support.

REFERENCES

[1] J. Deng, W. Dong, Y. Guo, X. Chen, R. Zhou, and W. Liu, "A novel remote sensing image enhancement method, the pseudo-tasseled cap transformation: Taking buildings and roads in GF-2 as an example," Appl. Sci., vol. 13, no. 11, p. 6585, 2023.

[2] P. M. Mather, Computer Processing of Remote-Sensed Images. New York: John Wiley & Sons, 1999.

[3] Z. Oleiwi, K. Thanoon, and K. Alsaif, "High frequency coefficient effect on image based on contourlet transformation," in Proc. IEEE Int. Conf. Comput. Inf. Sci. Technol. Appl. (ICCISTA), 2019.

[4] S. Oguzhanoglu, I. Kapucuoglu, and F. Sunar, "Comparison of satellite image denoising techniques in spatial and frequency domains," Int. Arch. Photogramm. Remote Sens. Spatial Inf. Sci., vol. XLIII-B3-2022, pp. 1241-1247, 2022.

[5] B. Zhang, M. Wang, and X. Shen, "Image haze removal algorithm based on nonsubsampled contourlet transform," IEEE Access, vol. 9, pp. 21708-21720, 2021.

[6] M. A. Al-Obaidi and Y. K. Al-Timimi, "Change detection in Mosul dam lake, north of Iraq using remote sensing and GIS techniques," Iraqi J. Agric. Sci., vol. 53, no. 1, pp. 38-47, 2022.

[7] A. Al-Hussein and A. Al-Hamadani, "Hydromorphological study of regulating lake of Mosul Dam, North Mosul City, Iraq," Iraqi Nat. J. Earth Sci., vol. 20, no. 1, pp. 20-30, 2020.

[8] N. Al-Ansari, N. Adamo, M. R. Al-Hamdani, K. Sahar, and R. E. A. Al-Naemi, "Mosul dam problem and stability," Engineering, vol. 13, no. 3, pp. 105-124, 2021.

[9] M. F. Yass and A. Al-Tikrite, "Sediment characteristics of the riverbed: The Tigris River case (Iraq)," Math. Model. Eng. Probl., vol. 12, no. 6, 2025.

[10] L. G. Linck, P. Gamba, and A. Garzelli, "Enhancing spatial resolution of Sentinel-2 next generation imagery via image fusion," IEEE J. Sel. Top. Appl. Earth Obs. Remote Sens., 2025.

[11] T. Zhang, J. Su, C. Liu, W.-H. Chen, H. Liu, and G. Liu, "Band selection in Sentinel-2 satellite for agriculture applications," in Proc. 23rd Int. Conf. Autom. Comput. (ICAC), 2017.

[12] T. Trongtirakul, D. Ladyzhensky, W. Chiracharit, and S. Agaian, "Non-linear contrast stretching with optimizations," in Mobile Multimedia/Image Processing, Security, and Applications 2019, vol. 10993, p. 1099303, SPIE, May 2019.

[13] M. N. Do and M. Vetterli, "Thermal barrier coatings: Improving thermal protection," Aircraft Eng. Aerosp. Technol., vol. 74, no. 4, pp. 72-73, 2002.

[14] K. I. Alsaif and M. M. Salih, "Contourlet transformation for text hiding in HSV color image," Int. J. Comput. Netw. Commun. Secur., vol. 1, no. 4, pp. 132-139, 2013.

[15] Z. N. A. Al-Rawi, H. R. Hatem, and I. H. Ali, "Image compression using contourlet transform," in Proc. 1st Annu. Int. Conf. Inf. Sci. (AiCIS), 2018.

[16] K. Chen, G. Zhang, C. Tang, Q. Ran, L. Wen, S. Han, and H. Yi, "Non-subsampled contourlet transform-based domain feedback information distillation network for suppressing noise in seismic data," Appl. Sci., vol. 15, no. 12, p. 6734, 2025.

[17] C. N. P. G. Arachchige and L. A. Prendergast, "Confidence intervals for median absolute deviations," Commun. Stat. Simul. Comput., pp. 1-10, 2024.

[18] V. Choulakian and G. Abou-Samra, "Mean absolute deviations about the mean, the cut norm and taxicab correspondence analysis," Open J. Stat., vol. 10, no. 1, pp. 97-112, 2020.

[19] N. Li, M. Ge, L. Wang, M. Unoki, S. Li, and J. Dang, "Global signal-to-noise ratio estimation based on multi-subband processing using convolutional neural network," in Proc. INTERSPEECH, pp. 361-365, 2022.

[20] X. Yang, J. Bryan, K. Okubo, C. Jiang, T. Clements, and M. A. Denolle, "Optimal stacking of noise cross-correlation functions," Geophys. J. Int., vol. 232, no. 3, pp. 1600-1618, 2023.